Contact radius of stamps in reversible adhesion

Jian Wu,[1] Seok Kim,[2] Andrew Carlson,[2] Chaofeng Lu,[1,3] Keh-Chih Hwang,[4] Yonggang Huang,[1, a)] and John A. Rogers[2, b)]

[1)] *Department of Civil and Environmental Engineering and Department of Mechanical Engineering, Northwestern University, Evanston, Illinois 60208*
[2)] *Department of Materials Science and Engineering, Beckman Institute, and Seitz Materials Research Laboratory, University of Illinois at Urbana-Champaign, Urbana, Illinois 61801*
[3)] *Department of Engineering Mechanics, Zhejiang University, Hangzhou, Zhejiang 310027, China*
[4)] *Department of Engineering Mechanics, Tsinghua University, Beijing 100084, China*

(Received 3 September 2010; accepted 23 November 2010; published online 10 January 2011)

Abstract A mechanics model is developed for the contact radius of stamps with pyramid tips in transfer printing. This is important to the realization of reversible control of adhesion, which has many important applications, such as climbing robots, medical tapes, and transfer printing of electronics. The contact radius is shown to scale linearly with the work of adhesion between the stamp and the contacting surface, and inversely with the plane-strain modulus of the stamp. It also depends on the cone angle and tip radius of the stamp, but is essentially independent of details of the tip geometry. © *2011 The Chinese Society of Theoretical and Applied Mechanics.* [doi:10.1063/2.1101101]

Keywords contact mechanics, reversible adhesion, contact radius

Geckos can climb on almost any surface because their feet have fibrillar structures to adjust adhesion with a surface. This has motivated extensive studies on biomimetic adhesion materials.[1–9] However, fibrillar structures are rather difficult to fabricate for synthetic materials. Inspired by aphids, which use sagging and retraction of foot pads to enlarge or diminish contact area with a surface to modulate adhesion, Kim *et al.*[10] (2010) developed a robust approach of reversible control of adhesion by adjusting the contact area with a surface. They fabricated a square polydimethysiloxane (PDMS) stamp with pyramid-shaped structures at each corner to pick up silicon platelets (or thin devices) from their growth substrate, and print (release) them onto a receiving substrate. When the PDMS stamp was pressed firmly against a silicon platelet, the entire stamp (including pyramids) collapsed onto the platelet to reach maximum contact area. The rapid retrieval of the PDMS stamp then picked up the platelet, after which the pyramids gradually resumed their original shape, leaving only their tips in contact with the platelet and therefore very small contact area. The platelet was then easily transferred to a receiving surface.

This approach has been demonstrated to successfully transfer print silicon platelets and membranes onto rough or non-adhesive surfaces, and fabricate an unusual transistor consisting of a printed gate electrode, a nanoscale air gap dielectric, and an aligned array of single walled carbon nanotubes.[10] The reversible control of adhesion is important to the development of climbing robots, medical tapes, and stamps for transfer printing.

The pyramid tip radius should be very small such that the stamp/platelet contact area is also very small upon stamp retraction. However, there is a limit for the tip radius, below which any sharper tips do not further reduce the contact area because of the adhesion between the stamp and platelet. The purpose of this letter is to determine the contact radius, which is important to pyramid (stamp) fabrication because any further sharpening of the tip becomes ineffective.

Figure 1(a) illustrates the surface of an axisymmetric tip, which has a conical portion with cone angle θ, and a spherical portion with tip radius $R_{\rm tip}$ and tip angle (angle of the spherical portion) $\theta_{\rm tip}$. The limit $\theta_{\rm tip} = \theta$ corresponds to a smooth tip, i.e. a continuous slope across the conical and spherical portions studied by Kim *et al.*.[10] The other limit $\theta_{\rm tip} = 180^\circ$ represents a sharp tip, which is equivalent to $R_{\rm tip} = 0$.

As illustrated in Fig. 1(b), contact with the silicon platelets causes the tips to deform to maintain equilibrium between attraction from surface adhesion and elastic repulsion, even without any applied load. These deformations lead to contact radius $R_{\rm contact}$ that may be considerably larger than $R_{\rm tip}$ such that further sharpening of the tip (decrease in $R_{\rm tip}$) would not reduce the contact area.

The surface in Fig. 1(a) is given in the cylindrical coordinates (r,z) by

$$z = f(r) = \begin{cases} R_{\rm tip} - \sqrt{R_{\rm tip}^2 - r^2}, \\ \quad 0 \le r \le R_{\rm tip}\cos\dfrac{\theta_{\rm tip}}{2}, \\ \dfrac{r}{\tan\dfrac{\theta}{2}} - R_{\rm tip}\left(\dfrac{\cos\dfrac{\theta-\theta_{\rm tip}}{2}}{\sin\dfrac{\theta}{2}} - 1\right), \\ \quad r > R_{\rm tip}\cos\dfrac{\theta_{\rm tip}}{2}. \end{cases} \tag{1}$$

Across the interface $r = R_{\rm tip}\cos\dfrac{\theta_{\rm tip}}{2}$ between the spherical and conical portions the slope is discontinuous and changes from $\theta_{\rm tip}$ to θ.

a) Corresponding author. E-mail: y-huang@northwestern.edu.
b) E-mail: jrogers@uiuc.edu

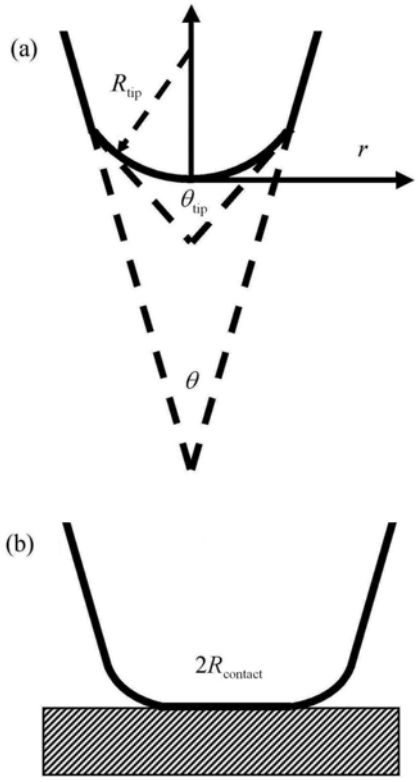

Fig. 1. (a) A schematic diagram of the surface of an axisymmetric tip, which has a conical portion with cone angle θ, and a spherical portion with tip radius R_{tip} and tip angle θ_{tip}; (b) a schematic diagram of the contact with contact radius $R_{contact}$

Classical models of contact mechanics[11] relates the contact radius $R_{contact}$ to the plane-strain modulus $\overline{E}$ of the stamp and the work of adhesion γ between the stamp and silicon platelets by

$$\frac{\overline{E}R_{contact}}{2\pi}\left[\frac{\delta}{R_{contact}}-\int_0^{R_{contact}}\frac{f'(r)\,dr}{\sqrt{R_{contact}^2-r^2}}\right]^2=\gamma, \quad (2)$$

for any surface shape $f(r)$, where δ is given by

$$\delta=\frac{1}{R_{contact}}\int_0^{R_{contact}}\sqrt{R_{contact}^2-r^2}f'(r)\,dr, \quad (3)$$

for vanishing applied load. The substitution of Eq. (3) into Eq. (2) gives the following equation for $R_{contact}$

$$\frac{\overline{E}}{2\pi R_{contact}^3}\left[\int_0^{R_{contact}}\frac{r^2f'(r)\,dr}{\sqrt{R_{contact}^2-r^2}}\right]^2=\gamma, \quad (4a)$$

or equivalently

$$R_{contact}\left[\int_0^1\frac{t^2f'(R_{contact}t)\,dt}{\sqrt{1-t^2}}\right]^2=\frac{2\pi\gamma}{\overline{E}}. \quad (4b)$$

The value of $R_{contact}$ scales linearly with the work of adhesion γ between the stamp and the contacting surface, and inversely with the plane-strain modulus $\overline{E}=E/(1-\nu^2)$ of the stamp (E—Young's modulus, $\nu\approx0.5$—Poisson's ratio)

For weak adhesion, contact remains in the spherical portion, $R_{contact}\le R_{tip}\cos\frac{\theta_{tip}}{2}$. Equation (4a) for $R_{contact}$ becomes

$$(\eta^2+1)\ln\frac{\eta+1}{\eta-1}-2\eta-4\sqrt{\frac{2\pi\gamma}{\overline{E}R_{tip}}}\sqrt{\eta}=0, \quad (5)$$

which is identical to Maugis[11] for a sphere, where $\eta=R_{tip}/R_{contact}$. The resulting contact radius, normalized by $\gamma/\overline{E}$, depends only on the normalized tip radius $R_{tip}/\gamma/\overline{E}$, and is given in Fig. 2. The substitution of $R_{contact}\le R_{tip}\cos\frac{\theta_{tip}}{2}$ into the above equation gives the requirement for the weak adhesion,

$$\gamma\le\overline{E}R_{tip}\left[\left(1+\cos^2\frac{\theta_{tip}}{2}\right)\ln\left(\tan\frac{\theta_{tip}}{4}\right)+\cos\frac{\theta_{tip}}{2}\right]^2\Big/\left(8\pi\cos^3\frac{\theta_{tip}}{2}\right).$$

For relatively strong adhesion, contact reaches the conical portion, $R_{contact}>R_{tip}\cos\frac{\theta_{tip}}{2}$. Equation (4a) for $R_{contact}$ becomes

$$\left(1+\eta^2\right)\ln\frac{1+\eta}{\sqrt{1-\eta^2\cos^2\frac{\theta_{tip}}{2}}+\eta\sin\frac{\theta_{tip}}{2}}-\eta+\frac{\cos\frac{\theta-\theta_{tip}}{2}}{\sin\frac{\theta}{2}}\eta\sqrt{1-\eta^2\cos^2\frac{\theta_{tip}}{2}}+\frac{\cos^{-1}\left(\eta\cos\frac{\theta_{tip}}{2}\right)}{\tan\frac{\theta}{2}}-2\sqrt{\frac{2\pi\gamma}{\overline{E}R_{tip}}}\sqrt{\eta}=0. \quad (6)$$

It degenerates to Kim *et al.*[10] for $\theta_{tip}=\theta$ (smooth tip). The relatively strong adhesion requires

$$\gamma>\overline{E}R_{tip}\left[\left(1+\cos^2\frac{\theta_{tip}}{2}\right)\ln\left(\tan\frac{\theta_{tip}}{4}\right)+\cos\frac{\theta_{tip}}{2}\right]^2\Big/\left(8\pi\cos^3\frac{\theta_{tip}}{2}\right).$$

The normalized contact radius $R_{contact}/(\gamma/\overline{E})$ depends on the normalized tip radius $R_{tip}/(\gamma/\overline{E})$, cone angle θ and tip angle θ_{tip}. For the limit of vanishing tip radius $R_{tip}\to0$ (or equivalently $\theta_{tip}=\pi$), Eq. (6) gives an asymptote

$$R_{contact}^{min}=\frac{32\gamma}{\pi\overline{E}}\tan^2\frac{\theta}{2}, \quad (7)$$

which is the minimal contact radius even for an atomistically sharp tip.

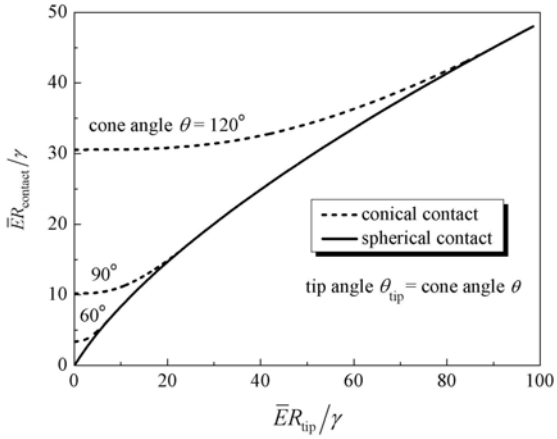

Fig. 2. The normalized contact radius, $\overline{E}R_{\text{contact}}/\gamma$, versus the normalized tip radius, $\overline{E}R_{\text{tip}}/\gamma$, for tip and cone angles $\theta_{\text{tip}} = \theta = 60^\circ$, 90° and 120°, where γ is the work of adhesion between the stamp and the contacting surface, and $\overline{E}$ is the plane-strain modulus of stamp.

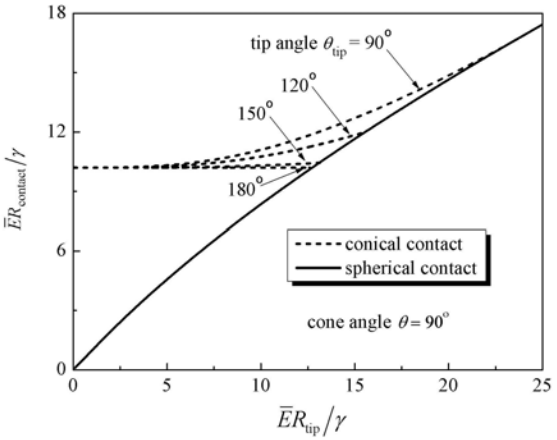

Fig. 3. The normalized contact radius, $\overline{E}R_{\text{contact}}/\gamma$, versus the normalized tip radius, $\overline{E}R_{\text{tip}}/\gamma$, for cone angle $\theta = 90^\circ$ and tip angle $\theta_{\text{tip}} = 90^\circ$ (smooth tip), 120°, 150° and 180° (sharp tip), where γ is the work of adhesion between the stamp and the contacting surface, and $\overline{E}$ is the plane-strain modulus of stamp.

Figure 2 shows the normalized contact radius, $\overline{E}R_{\text{contact}}/\gamma$, versus the normalized tip radius, $\overline{E}R_{\text{tip}}/\gamma$, for$\theta_{\text{tip}} = \theta = 60^\circ$, 90° and 120°. The solid line and dashed lines represent spherical and conical contact, respectively. The contact radius decreases with the tip radius, but the decrease is much slower in conical contact than in spherical contact, and approaches the asymptote in Eq. (7) as $R_{\text{tip}} \to 0$. For a given tip radius, however, the contact radius decreases rapidly with the cone angle (during conical contact) such that a sharp cone is effective to reduce the contact area.

Figure 3 shows the normalized contact radius, $\overline{E}R_{\text{contact}}/\gamma$, versus the normalized tip radius, $\overline{E}R_{\text{tip}}/\gamma$, for cone angle $\theta = 90^\circ$ and different tip angle $\theta_{\text{tip}} = 90^\circ$ (smooth tip), 120°, 150° and 180° (sharp tip). For a given tip radius, the contact radius (in conical contact) decreases with the increase of tip angle θ_{tip}; a smooth tip gives the maximum contact radius, while Eq. (7) gives the minimal contact radius. Their difference, however, is rather small. This suggests that the contact radius, normalized by $\gamma/\overline{E}$, depends on the cone angle θ and tip radius R_{tip}, and is approximately independent of the detailed tip geometry.

It should be pointed out that, for a smooth tip $\theta_{\text{tip}} = \theta$, the contact radius obtained from Eq. (6) agrees well with the finite element analysis and experiments[10]. For non-smooth tips ($\theta_{\text{tip}} \neq \theta$) the contact radius is essentially independent of details of the tip geometry, and depends only on the cone angle θ and tip radius R_{tip}. The contact radius during transfer printing in reversible adhesion scales linearly with the work of adhesion γ between the stamp and the contacting surface, and inversely with the plane-strain modulus of the stamp.

1. A. K. Geim, S. V. Dubonos, I. V. Grigorieva, K. S. Novoselov, A. A. Zhukov, and S. Y. Shapoval, Nature Materials **2**, 461 (2003).
2. M. Sitti and R. S. Fearing, J. Adhesion Science and Technology **17**, 1055 (2003).
3. H. Gao and H. Yao, Proc. Natl. Acad. Sci. U.S.A. **101**, 7851. (2004)
4. S. Kim and M. Sitti, Appl. Phy. Lett. **89**, 261911 (2006).
5. S. Gorb, M. Varenberg, A. Peressadko, and J. Tuma, J. of the Royal Society Interface **4**, 271 (2007).
6. S. Reddy, E. Arzt, and A. del Campo, Advanced Materials **19**, 3833 (2007).
7. J. Lee and R. S. Fearing, Langmuir **24**, 10587 (2008).
8. M. P. Murphy, B. Aksak, and M. Sitti, Small **5**, 170 (2009).
9. S. Kim, M. Sitti, T. Xie, and X. Xiao, Soft Matter **5**, 3689 (2009).
10. S. Kim, J. Wu, A. Carlson, S. H. Jin, A. Kovalsky, P. Glass, Z. Liu, N. Ahmed, S. L. Elgan, W. Chen, P. M. Ferreira, M. Sitti, Y. Huang, and J. A. Rogers, Proc. Natl. Acad. Sci. U.S.A. 107, 17095 (2010).
11. D. Maugis, Langmuir **11**, 679 (1995).